# Research on Foreign Object Detection Technology in Wireless Charging System for Electric Vehicles

Liu Changke
School of Mechanical Engineering
Xi`an Technological University
Xi'an, China
E-mail: liuchangke@foxmail.com

Lai Hao
Academy of Aerospace Solid Propulsion Technology
AASPT
Xi'an, China
E-mail: 15909200228@163.com

Shang Yaceng
School of Mechanical Engineering
Xi`an Technological University
Xi'an, China
E-mail: 13279376583@163.com

Sun Kaidong
School of Mechanical Engineering
Xi`an Technological University
Xi'an, China
E-mail: 1356058684@qq.com

***Abstract*—Foreign object detection is an important issue that restricts the development of wireless charging for electric vehicles. When foreign matter enters the charging area during charging, the impedance of the charging coil changes. According to this principle, the result shows that the higher the coil excitation frequency, the more obvious the coil impedance changes. In order to carry out accurate foreign object detection while charging, this paper proposes a dual-frequency inductive charging method. The high frequency is used for foreign object detection, the low frequency is used for wireless charging, the power supply topology and design method are given, and the simulation is verified.**

***Keywords-Wireless Charging; Dual-Frequency; Foreign Object Detection***

## I. INTRODUCTION

At present, the research on electric vehicle charging system is developing rapidly. Compared with the traditional plug-in charging method, wireless charging has attracted more and more attention from researchers and enterprises due to its convenience and security [1-6]. Wireless charging transmits electrical energy from the transmitting coil to the receiving coil through the principle of electromagnetic induction, which is convenient, safe and environmentally friendly. However, when there is a metal foreign matter such as a can, a coin, or the like between the transmitting coil and the receiving coil, the metal is heated by the magnetic field, which may cause a safety problem such as a fire in the vehicle.

The foreign matter detection method used in this paper is the impedance method. It is shown by experiments that the higher the frequency of excitation of the coil, the greater the variation of the impedance of the coil after the foreign matter enters, that is, the better the detection effect. In order to balance the charging and detection effects, this paper proposes a dual-frequency induction wireless charging method, high frequency for foreign object detection and low frequency for wireless charging. The power supply topology and design method are given in the paper, and the simulation is verified.

## II. FOREIGN BODY DETECTION EXPERIMENT

### A. Detection incentive

The change in impedance of the circular coil and the DD coil is measured using a bridge. The bridge applies an excitation signal to the transmitting coil, and an alternating magnetic field is generated on the surface of the transmitting coil. After the foreign matter enters, the impedance of the transmitting coil can be changed. The principle of bridge detection is shown in Figure 1:

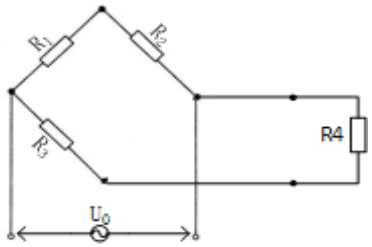


Figure 1. LCL resonant circuit

$R_1$, $R_2$, and $R_3$ are known impedances and are located inside the bridge measuring instrument. $R_4$ is the impedance of the coil to be tested and is connected to two external terminals of the bridge.

### B. Experimental result

In this experiment, the change of the coil impedance is caused by the foreign matter entering the coil magnetic field range. The coils used are as shown in Figure. 2, which are a circular coil and a DD coil, respectively. Foreign objects use common metals and hands, as shown in Figure 3.

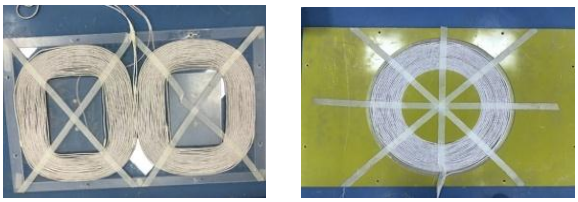

(a) DD coil (b) Circular coil

Figure 2. Coil model

(a) Copper sheet (b) Iron block


(c) Cans

Figure 3. Foreign body type

The bridge model is: MS5308LCR digital bridge. There are five kinds of frequency changes in the internal excitation source, which a 100Hz/120Hz/1kHz/10kHz/100kHz. Shown in Figure 4.

Figure 4. Bridge

Table 1 and Table 2 are the impedance values of the coil when the foreign signal enters the magnetic field of the coil when the signal source frequency is 1KHz, 10KHz and 100Khz, respectively, and the average value of each foreign object is measured three times at different frequencies to increase the accuracy.

TABLE I. CIRCULAR COIL IMPEDANCE CHANGE

| | 1KHz | 10KHz | 100KHz |
|---|---|---|---|
| Copper sheet | 0. 003 | 0. 022 | 0. 328 |
| Iron block | 0. 03 | 0. 191 | 1. 016 |
| Cans | 0. 014 | 0. 084 | 0. 655 |
| Hand | 0. 001 | 0. 005 | 0. 477 |

TABLE II. DD COIL IMPEDANCE CHANGE

| | 1KHz | 10Khz | 100KHz |
|---|---|---|---|
| Copper sheet | 0. 001 | 0. 005 | 0. 006 |
| Iron block | 0. 009 | 0. 049 | 0. 176 |
| Cans | 0. 002 | 0. 028 | 0. 081 |
| Hand | 0 | 0. 001 | 0. 017 |

The impedance changes obtained in Tables 1 and 2 are plotted as a line graph, as shown in Figures 5 and 6.

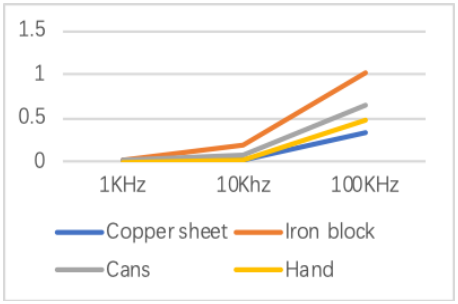


Figure 5. Circular coil impedance change line diagram

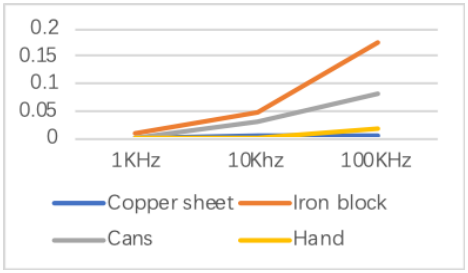


Figure 6. DD coil impedance change line diagram

It can be seen from the drawn line graph that the coil impedance changes caused by foreign matter at different frequencies are different, and the higher the frequency, the more obvious the impedance change. The iron block has the greatest influence on the impedance of the coil, and the DD coil has good repeatability when measuring the impedance. Under the same number of turns, the foreign matter enters the DD coil to cause a small change in impedance and has little influence on the performance parameters of the coil.

However, the current wireless charging frequency is generally between 20KHz and 100KHz. When the foreign matter enters within 100KHz, the impedance change of the coil is not obvious. Therefore, in order to balance the charging and detection effects, this paper proposes a dual-frequency induction wireless charging method. Foreign object detection, low frequency for wireless charging.

## III. DUAL FREQUENCY INDUCTION WIRELESS CHARGING CIRCUIT DESIGN

The dual-frequency topology designed in this paper is shown in figure7. The high and low excitation sources can be applied to the transmitting coil at the same time, and a high-frequency resonant current and a low-frequency resonant current can be obtained on the transmitting coil.

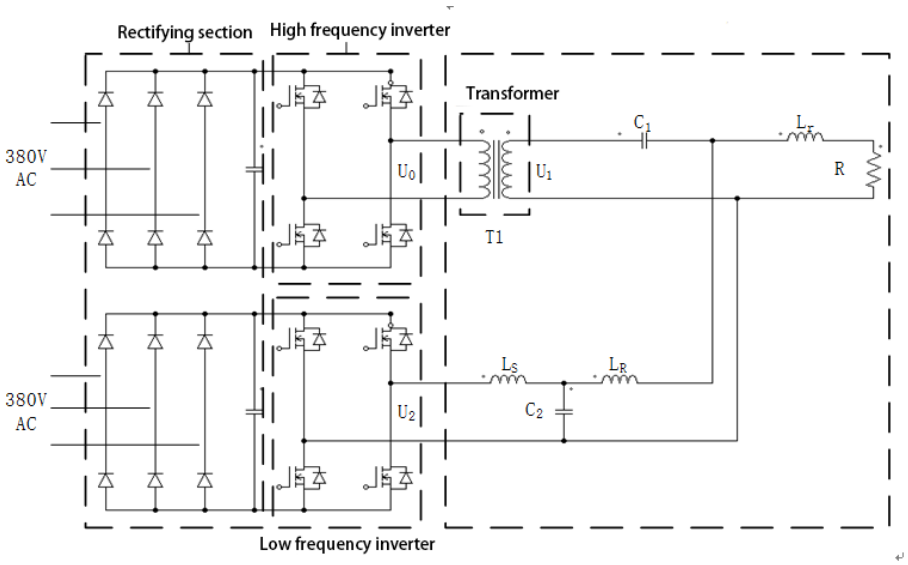


Figure 7. Dual-frequency induction wireless charging main circuit diagram figure

### A. *High frequency circuit parameter design*

High-frequency excitation is used to achieve foreign object detection, using an inverter with a power of 1kW and a frequency of 1MHz. The equivalent circuit diagram of the high frequency resonant tank circuit is shown in Figure 8.

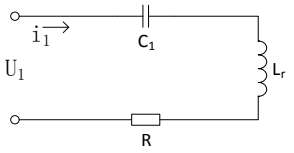


Figure 8. High frequency resonant tank equivalent diagram

The impedance $Z_1$ of the equivalent circuit is:

$$Z_1(\omega_H) = R + j(\omega_H L_r - \frac{1}{\omega_H C_1}) \tag{1}$$

Reactance of the loop:

$$X = \omega_H L_r - \frac{1}{\omega_H C_1} \tag{2}$$

When the circuit resonates:

$$\omega_H L_r = \frac{1}{\omega_H C_1} \tag{3}$$

The value of the high frequency resonant capacitor C1 of the formula (3) is：

$$C_1 = \frac{1}{\omega_H^2 L_r} = 46.9nF \tag{4}$$

The transformer $T_1$ ratio is

$$T_1 = \frac{U_H}{\sqrt{P_H \cdot R}} = 36 \tag{5}$$

### B. *Low frequency circuit parameter design*

The low frequency excitation is used for power transmission. The inverter uses a charging power of 5kW and a frequency of 100kHz. The low frequency part circuit can be equivalent to the LCL structure shown in Figure 9。 Among them $L_E = L_R + L_r$.

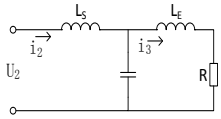


Figure 9. LCL resonant ciricut

The impedance $Z_2$ expression of the LCL circuit is：

$$Z_2(\omega) = j\omega Ls + \left[ j\omega C_2 + (j\omega L_E + R)^{-1} \right]^{-1} \tag{6}$$

The phase and amplitude characteristics of the load can be derived from equation (6). There are two resonance points in the loop, the series resonance point and the parallel resonance point.

$$\omega_0 = \frac{1}{\sqrt{\frac{L_S L_E}{L_S + L_E} C_2}} \tag{7}$$

$$\omega_1 = \frac{1}{\sqrt{L_E C_2}} \tag{8}$$

Among them $\omega_0 < \omega_1$. The low frequency inverter uses a voltage type inverter, so the circuit should work in a weakly inductive state, which is the ideal frequency operating point. Define the following variables

$$Q_L = \frac{1}{R}\sqrt{\frac{L_S L_E}{L_S + L_E}} \quad (9)$$

$$\beta = \frac{L_S}{L_E} \quad (10)$$

Then, when the circuit operates at the resonance point, the impedance expressions obtained by equations (5), (6), (8), and (9) are:

$$Z_2(\omega_0) = Q_L R\beta^2 \frac{1}{Q_L - j\beta} \quad (11)$$

$U_2$ is the output voltage of the low frequency inverter. When the resonant frequency of the load is close to the series resonant frequency, the output power of the power supply is maximized at the same time [7]. The maximum output power can be expressed as:

$$P_{\max} = \frac{U_2^2}{2}\mathrm{Re}\left[\frac{1}{Z(\omega_0)}\right] \approx \frac{U_2^2}{2R\beta^2} \quad (12)$$

From equations (11):

$$\beta = \sqrt{\frac{U_2^2}{2RP_L}} \approx 11 \quad (13)$$

From equations (6) and (8):

$$C_2 = \frac{1}{\omega_0 R Q_L} = 0.35\mu F \quad (14)$$

From equations (6)，(8) and (10):

$$L_E = \frac{(1+\beta)Q_L R}{\omega_0 \beta} = 7.7uH \quad (15)$$

From equations (9):

$$L_S = \beta L_R = 84.7uH \quad (16)$$

At this point, the parameters in the circuit have been determined.

## IV. CROSSTALK CURRENT ANALYSIS AT THE OUTPUT OF HIGH AND LOW FREQUENCY INVERTERS

In the dual-frequency topology, interference occurs between the two inverter circuits due to the formation of a path between the high-frequency inverter circuit and the low-frequency inverter circuit. In severe cases, it may affect the normal operation of the system. Therefore, the influence of streaming is an important indicator of the design of this circuit. The equivalent circuit diagram of the dual-frequency induction main circuit topology in high and low frequency modes is shown in Figure 10 and Figure 11.

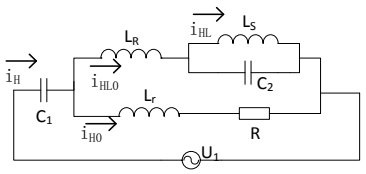


Figure 10. Equivalent circuit diagram in high frequency mode

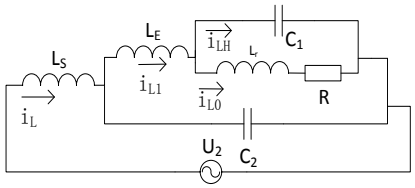


Figure 11. Equivalent circuit diagram in low frequency mode

In order to the inverter to work properly, the crosstalk current flowing into the inverter should be sufficiently smaller than its own output current, and the superimposed waveform still has only one zero crossing in half cycle. In the half cycle, the low frequency circuit has:

$$|i_L| > |i_{HL}| \quad (17)$$

The $i_L$ is the output current of the low frequency inverter $i_L = I_L \sin\omega_L t$ ， $i_{HL}$ is the crosstalk current that the high frequency current flows into the output of the low frequency inverter， $i_{HL} = I_{HL}\sin\omega_H t$ 。

$$|I_L \sin\omega_L t| > |I_{HM}\sin\omega_H t| \quad (18)$$

From equations (18):

$$\frac{I_{HL}}{I_L} < \left|\frac{\sin\omega_L t}{\sin\omega_H t}\right| \quad (19)$$

In the half low frequency period:

$$\left|\frac{\sin\omega_L t}{\sin\omega_H t}\right| \geq \frac{\omega_L}{\omega_H} \quad (20)$$

$$\frac{\omega_L}{\omega_H} = \frac{2\pi\times10^5}{2\pi\times10^6} = 10\% \quad (21)$$

So, for low frequency circuits： $\frac{I_{HL}}{I_L} < 10\%$ 。Similarly, for high frequency circuits： $\frac{I_{LH}}{I_H} < 10\%$ 。

According to the above analysis, if the crosstalk current entering the output terminals of the high and low frequency inverters is less than 10% of the inverter's own output current, the output currents of the high and low frequency inverters still have the original periodicity.

## V. SIMULATION EXPERIMENT

In the dual-frequency system, the current waveforms at the output are shown in Figure 12(a) and Figure 12(b).

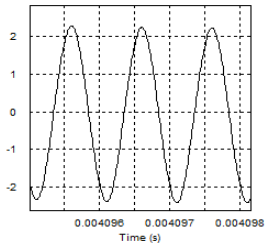


High-frequency inverter output current simulation waveform

（a）

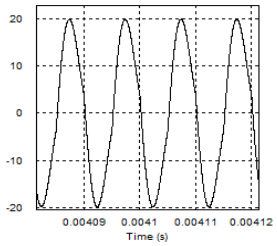


Low frequency inverter output current simulation waveform

（b）

Figure 12. Inverter output current waveform

It can be seen from the figure that the currents at the output of the high and low frequency inverters are both sinusoidal and in resonance. Figure 13(a) and Figure 13(b) are FFT analysis diagrams of the current at the output of the high and low frequency inverters, respectively. Among them, the high-frequency inverter output current is 1.99A, the low-frequency component flowing into the output end of the high-frequency inverter is 0.064A; the cross-talk current accounts for 3.2% of the output current of the high-frequency inverter; the output current of the low-frequency inverter For 13.28A, the high-frequency current component flowing into the low-frequency inverter is 0.009A, and the crosstalk current accounts for 0.06% of the output current of the low-frequency inverter, which does not affect the original cycle.

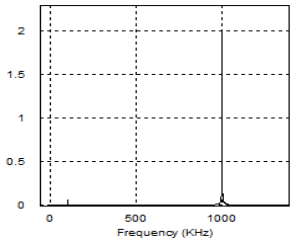


FFT analysis of the current at the output of the high frequency inverter

（a）

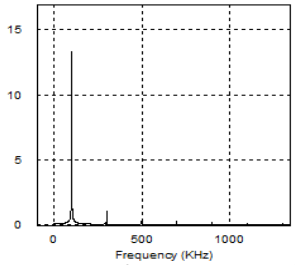


FFT analysis of the output current of the low frequency inverter

（b）

Figure 13. Inverter output current FFT analysis diagram

Figure 14 shows the load current simulation waveform diagram and the load current waveform FFT analysis diagram.

It can be seen from the two graphs that the load current waveform is superimposed with high and low frequency currents, and exhibits sinusoidal periodic oscillation, realizing synchronous dual-frequency output.

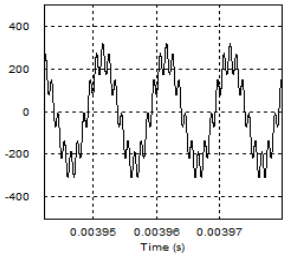


Load current simulation waveform

(a)

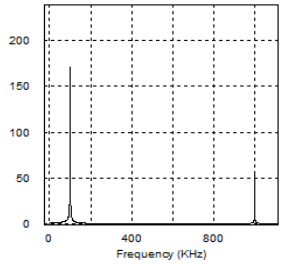


Load current simulation waveform FFT analysis chart

(b)

Figure 14. Circuit waveform on the load coil

## VI. CONCLUSIONS

Through the experiment based on the impedance method, it is found that the higher the coil excitation frequency, the more obvious the impedance change of the coil after the foreign matter enters. In order to balance the charging and detection effects, this paper proposes a dual-frequency induction wireless charging method. After theoretical analysis and simulation verification of the above circuit, this method can add high and low resonant currents on the transmitting coil. Through the stream analysis, it can be concluded that the inverter can output normally under this design scheme. Since the high frequency excitation only functions as a foreign object detection, the next step should be to further reduce the power of the high frequency excitation within a reasonable range of influence of the stream.

## REFERENCES

[1] CHOI S Y, JIN H, LEE W Y, et al. Asymmetric Coil Sets for Wireless Stationary EV Chargers With Large Lateral Tolerance by Dominant Field Analysis [J]. 2014, 29(12): 6406-20.

[2] SU Y C, GU B W, LEE S W, et al. Generalized Active EMF Cancel Methods for Wireless Electric Vehicles [J]. 2014, 29(11): 5770-83.

[3] SU Y C, GU B W, JEONG S Y, et al. Advances in Wireless Power Transfer Systems for Roadway-Powered Electric Vehicles [J]. 2016, 63(10): 6533-45.

[4] PARK C, LEE S, CHO G H, et al. Innovative 5-m-Off-Distance Inductive Power Transfer Systems With Optimally Shaped Dipole Coils [J]. 2014, 30(2): 817-27.

[5] RIM C T, CHO G H J E L. New approach to analysis of quantum rectifier-inverter [J]. 1989, 25(25): 1744-5.

[6] COVIC G A, BOYS J T J I J O E, ELECTRONICS S T I P. Modern Trends in Inductive Power Transfer for Transportation Applications [J]. 2013, 1(1): 28-41.

[7] Li Jingang, Sun Qi, Liu Weiwu. Research on high frequency induction heating power supply based on load matching of LLC load resonant circuit [M]. Proceedings of the 12th Annual Conference of Institute of Power Electronics, China Electrotechnical Society. Harbin. 2010: 1-4.